

Experimental Effervescence and Freezing Point Depression Measurements of Nitrogen in Liquid Methane-Ethane Mixtures

I.A. Richardson^a, J.W. Hartwig^{b,*}, and J.W. Leachman^a

^a *Hydrogen Properties for Energy Research (HYPER) Laboratory, Washington State University, Pullman, WA 99164-2920 USA*

^b *Cryogenic Propulsion Engineer, NASA Glenn Research Center, Cleveland, OH 44106 USA*

Abstract. NASA is designing an unmanned submarine to explore the depths of the hydrocarbon-rich seas on Saturn's moon Titan. Data from Cassini indicates that the Titan north polar environment sustains stable seas of variable concentrations of ethane, methane, and nitrogen, with a surface temperature near 93 K. The submarine must operate autonomously, study atmosphere/sea exchange, interact with the seabed, hover at the surface or any depth within the sea, and be capable of tolerating variable hydrocarbon compositions. Currently, the main thermal design concern is the effect of effervescence on submarine operation, which affects the ballast system, science instruments, and propellers. Twelve effervescence measurements on various liquid methane-ethane compositions with dissolved gaseous nitrogen are thus presented from 1.5 bar to 4.5 bar at temperatures from 92 K to 96 K to simulate the conditions of the seas. After conducting effervescence measurements, two freezing point depression measurements were conducted. The freezing liquid line was depressed more than 15 K below the triple point temperatures of pure ethane (90.4 K) and pure methane (90.7 K). Experimental effervescence measurements will be used to compare directly with effervescence modeling to determine if changes are required in the design of the thermal management system as well as the propellers.

Keywords: Effervescence, Methane-Ethane Mixtures, Extraterrestrial Submarine, Titan, freezing point depression

1. Introduction

Saturn's moon Titan is the only known celestial body in our solar system besides Earth with stable liquid seas accessible on the surface (Stofan et al., 2007). NASA is currently designing an unmanned autonomous submarine to explore these methane-ethane rich seas: 1) to study the evolution of hydrocarbons in the universe, 2) to study Titan's geology (atmosphere/sea exchange, surface, shore, waves, heat transfer), and 3) to provide a pathfinder for later designs of submersibles in the seas hidden beneath the ice crust of other outer planetary moons (Hartwig et al., 2016). The submarine has the advantage of being able to conduct measurements of the atmosphere and seas.

* Corresponding author at: M/S: 301-3, NASA Glenn Research Center, Cleveland, OH 44135, USA Tel.: +1 216 433 3979.

E-mail address: Jason.W.Hartwig@nasa.gov (J.W. Hartwig).

39 Data from Cassini indicates that the surface temperature of Titan is approximately 93 K with an
40 atmospheric pressure of 1.5 bar (Mitri et al., 2007; Lorenz and Mitton, 2010). The seas vary in
41 the amount of liquid methane and ethane (Lorenz et al., 2014; Tokano and Lorenz, 2016). Unlike
42 the liquid water oceans of Earth, the hydrocarbon seas of Titan are able to absorb a relatively
43 substantial amount of nitrogen from the atmosphere, causing gaseous nitrogen to go into
44 solution. The solubility of nitrogen varies dramatically depending on the composition of ethane
45 and methane in the seas, which can vary from nearly pure ethane in Kraken Mare to 74 mol %
46 methane in Ligeia Mare (Hartwig et al., 2016). At Titan's surface conditions of 93 K and 1.5 bar,
47 the solubility of nitrogen in Ligeia Mare is estimated to be 12-13 mol % while the solubility of
48 nitrogen in Kraken Mare is estimated at just 3 mol % (Hartwig et al., 2017). This range in
49 solubility presents several design challenges and creates uncertainty regarding ice formation in
50 the seas due to Titan's surface temperature being within 2 K to 3 K of the triple point of pure
51 methane and ethane. Though there is limited experimental data, the literature suggests that
52 significant freezing point depression can be achieved, and that the buoyancy of the ice will
53 depend on the solubility of nitrogen and the methane-ethane composition of the sea (e.g.
54 Thompson, 1985; Roe and Grundy, 2012; Prokhvatilov and Yantsevich, 1983; Hofgartner and
55 Lunine, 2013). Even though the depth of Ligeia Mare is known to be relatively shallow at 200 m
56 (Mastrogiuseppe et al., 2014), it is unknown if the temperature gradient is enough to incite
57 freezing at these depths.

58
59 The primary thermal design concern of the submarine is predicting the effects of nitrogen
60 effervescence on submarine operation. The 350-400 W/m² waste heat flux from the submarine
61 radioisotope power system is not enough to boil the surrounding seas, but it may cause dissolved
62 nitrogen gas to come out of solution (Hartwig et al., 2016). In a quiescent case, bubbles may
63 interfere with sensitive science measurements. In a moving case, bubbles that form along the
64 body may coalesce at the aft end of the submarine and cause cavitation in the propellers. Due to
65 the high solubility of nitrogen in the Titan seas, data and models are needed to quantify the
66 amount of dissolved gas, as well as conditions that will cause bubbles to form, grow, and
67 coalesce along the submarine.

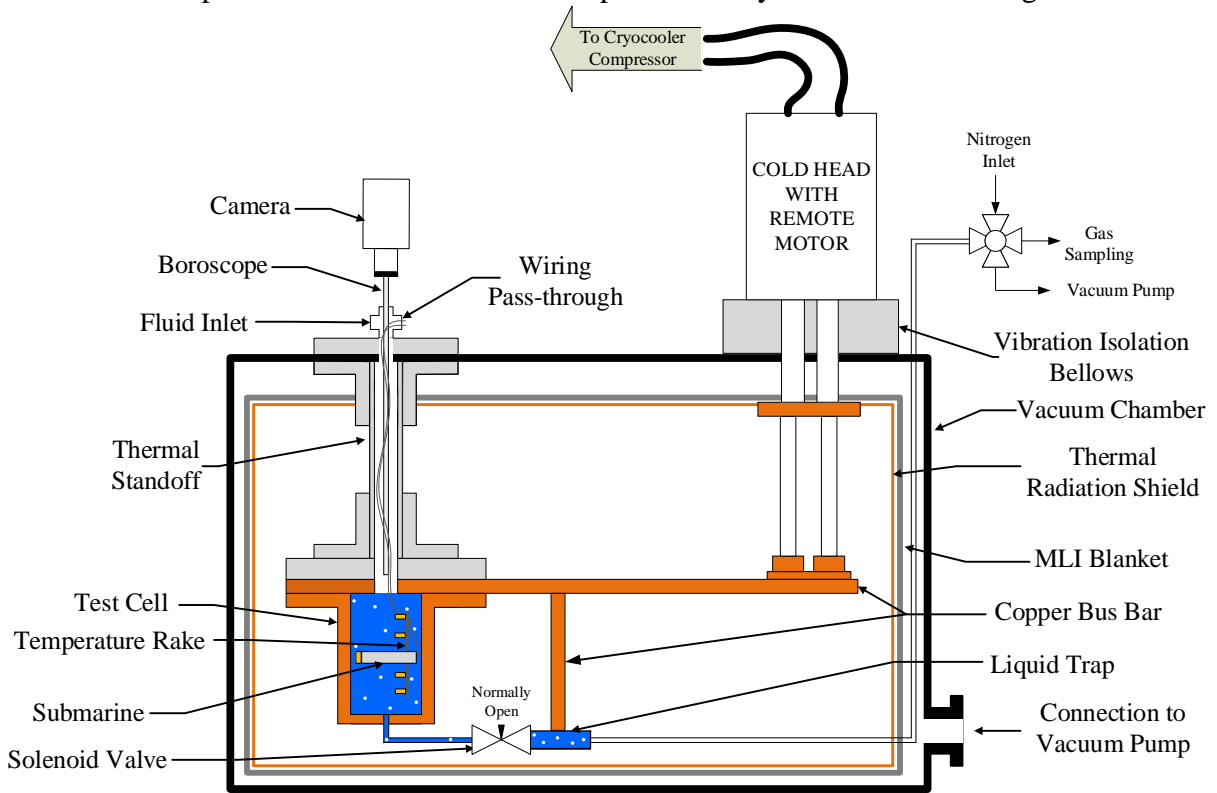
68
69 Effervescence and nitrogen dissolution in the seas of Titan has been modelled and discussed
70 previously with respect to composition change and bulk warming/cooling (Cordier et al., 2017;
71 Malaska et al., 2016). The current work focuses specifically on the effects of heat dissipation
72 from a Titan submarine. Experimental measurements were conducted to determine the heat
73 fluxes and surface temperatures at which nitrogen gas begins to come out of solution to
74 determine the point of bubble incipience as a function of sea temperature, pressure, and liquid
75 methane-ethane compositions. Videos of effervescence were taken to better understand the
76 impact that nitrogen gas bubbles may have on the scientific instruments and submarine
77 propellers. Additionally, two freezing point depression measurements were conducted on
78 methane-ethane-nitrogen mixtures to determine the degree of depression.

79

80 **2. Experimental Design**

81 The effervescence measurements presented in this work were completed using the same cryostat,
82 bulk gases, mixing tank, and liquid trap that were used to conduct pressure-density-temperature-
83 composition measurements on liquid methane-ethane-nitrogen mixtures relevant to Titan

84 (Richardson et al., 2018). The key components of the experimental system include a custom
 85 cryostat and test cell to condense methane-ethane mixtures, video camera with a borescope,
 86 cartridge heater to simulate waste heat from the submarine, and liquid trap which is used to
 87 determine the composition. A schematic of the experimental system is shown in Figure 1.



88
 89
 90 Figure 1. Experimental system used to conduct effervescence measurements.
 91

92 Gas cylinders of 99.99 % pure ethane and 99.99 % pure methane were mixed based on partial
 93 pressure in a mixing tank to achieve the approximate desired composition using Dalton's law.
 94 The gaseous mixture was then condensed via cryo-pumping in the copper test cell where
 95 nitrogen was bubbled in through the liquid trap at the bottom until the desired total pressure was
 96 achieved. Nitrogen bubbling was a turbulent process ensuring that the liquid mixture within the
 97 liquid trap and test cell was well mixed. The temperature of the test cell and liquid was
 98 controlled using a Proportional-Integral-Derivative (PID) temperature controller and electric
 99 heater placed on the outside of the test cell. The temperature controller supplied power to the
 100 heater to maintain a specified liquid temperature. Once the temperature and pressure of the
 101 simulated sea was stable, the cartridge heater was turned on to simulate the heat given off by the
 102 submarine. A summary of the sensors and instruments used to conduct the effervescence
 103 measurements is presented in Table 1.
 104

105 Table 1. Summary of instrumentation and sensors used to conduct effervescence measurements.

Measurement	Instrument	Accuracy
Pressure	Paroscientific Digiquartz®	0.01 %

	Pressure Transducer Model 1000-500A	
Liquid Temperature	LakeShore PT-100	± 0.25 K
Heater Surface Temperature	Cryo-con S950-BB (uncalibrated)	± 0.4 K
Composition	Varian CP-3800 GC	0.6 %
Heat Flux	HP 6438B DC Power Supply	± 0.25 V, ± 0.025 A

106
107
108
109
110
111
112
113
114

The temperature of the liquid was measured using a temperature rake which consists of four platinum resistance thermometers (PRT) vertically spaced approximately 2.5 cm apart. Two PRTs were located below the cartridge heater and two PRTs were above the heater. The bulk sea temperature was determined by averaging the two PRT measurements that were below the heater which generally agreed within 0.1 K. The PRTs above the heater were used to measure the thermal gradient that occurred above the heater due to natural convection.

115
116
117
118
119
120
121
122
123
124
125

The test cell had an internal diameter of 8.3 cm and a depth of 12.2 cm. The submarine was represented by a 5 cm long, 0.76 cm diameter cartridge heater. The heater surface temperature was measured by a silicon diode that was thermally anchored to the flat end of the heater. The power supplied to the heater was controlled using a DC power supply. Initial measurements were conducted at near steady state conditions by increasing the heater power in 2 volt increments and waiting at least 5 minutes until the liquid and heater temperature stabilized. If effervescence did not occur, heater power was increased in 2 volt increments until effervescence occurred. Later measurements were conducted by increasing the heater power rapidly; 2 volts every 30 seconds until effervescence occurred in order to minimize the effect of trace amounts of non-visible, dissolved gas coming out of solution during the progression towards effervescence. Additional information on the two measurement methods is provided in Section 3.

126
127
128
129
130
131
132
133

Effervescence was detected optically using a video camera and borescope as shown in Figure 1. The borescope allowed the video lens to pass into the test cell and maintain a hermetic seal. As a result, the end of the borescope was subject to the condition of the fluid being measured. This led to poor resolution for a few of the measurements due to fogging. A large uncertainty in the effervescence measurements is determining when effervescence occurs; similar to the different boiling regimes, there are varying degrees of effervescence. Effervescence was determined at the point of visible bubbles.

134
135
136
137
138
139

The composition of the liquid mixture at effervescence was obtained using a liquid trap. The liquid trap consisted of a section of brass pipe connected to the test cell through a 0.625 mm (0.25 inch) copper tube. A normally open solenoid valve was located between the test cell and the brass pipe allowing liquid to move freely between the liquid trap and the test cell. It was assumed that there was no stratification between the liquid in the test cell and the liquid trap

140 because of the turbulence caused by nitrogen bubbling. Once effervescence occurred, the
141 solenoid valve was closed separating the liquid in the trap from the liquid in the test cell. The
142 liquid in the liquid trap was heated until it was completely vaporized. Vaporization was ensured
143 by heating the liquid trap above the saturation temperature of liquid ethane, which is the highest
144 of the three components. The vapor was collected in a sampling cylinder. After the liquid was
145 completely vaporized, the gaseous mixture was extracted and collected in a 1 liter multilayer gas
146 sampling bag where it was analyzed via gas chromatography. For redundancy, three separate gas
147 sampling bags were filled and analyzed for the composition measurement for each data point. A
148 Varian CP-3800 GC system with a thermal conductivity detector was used to quantify nitrogen
149 and a flame ionization detector was used to quantify the methane and ethane gases. The gas
150 chromatograph utilizes a Silcosteel HaysSepQ 80/100 mesh packed column (5.5m X 3.175mm;
151 Supelco). The method used for this analysis incorporated a 10 μ L stainless steel injection loop
152 controlled by a Valco switching valve installed in the oven. The column oven was held isocratic
153 at 80 °C for 8 min, and the helium carrier gas had a 65 mL/min flow rate (1.448 bar).
154 Calibrations were made with certified standards (%v/v) of at least three levels for nitrogen (5 %
155 up to 20 %), methane and ethane (15 % up to 100 %) having a certified accuracy of 5 %. The
156 uncertainty associated with the certified gas standards and calibration curves were not accounted
157 for in the reported composition uncertainties. The linear calibration curves for methane, ethane,
158 and nitrogen had a coefficient of determination (R-squared value) greater than 0.9998 for each
159 component suggesting the uncertainty of the certified gas standards was much less than the
160 provided accuracy of 5 mol %. The only error considered in the reported composition
161 uncertainties is the standard deviation from conducting composition analysis in duplicate from
162 three gas sampling bags that were collected for each data point. The composition accuracy
163 reported in Table 1 was founded using the largest reported standard deviation.

164
165 The solenoid valve used in the liquid trap would occasionally experience leakage, which could
166 ultimately bias the composition of the measurements. Measurements with detectable leakage
167 have been noted. To reduce the effects of valve leakage, an effort was made to equalize the
168 pressure on each side of the valve to reduce the flow potential.

169

170 **3. Effervescence Measurements**

171 Measurements were conducted for liquid temperatures ranging from 92 K to 96 K and varying
172 methane-ethane-nitrogen compositions to cover the range of sea conditions that exist on Titan.
173 Pressures were varied from 1.5 bar to 4.5 bar to account for varying sea depths. The twelve
174 effervescence measurements and respective uncertainties are presented in Table 2. The reported
175 expanded uncertainties, $U = ku_c$ where u_c is the combined standard uncertainty, were
176 determined using a coverage factor of 2 ($k = 2$). Thus the expanded uncertainties have a 95%
177 level of confidence as recommend by the National Institute of Standards and Technology (Taylor
178 and Kuyatt, 1994). The individual uncertainties and sources of errors for each of the
179 experimental measurements have been discussed by Richardson (2017).

180

181 Table 2: Effervescence measurements of methane-ethane-nitrogen mixtures.

Measurement	Methane [mol %]	Ethane [mol %]	Nitrogen [mol %]	Pressure [bar]	Liquid Temp. [K]	Heater Surface Temp. [K]	Heat Flux at Bubble Incipience [kW/m ²]
1 ^a	87.1 ±0.3	0.0	12.9 ±0.3	1.546 ±0.007	96.2 ±0.5	101.4 ±0.8	10.830 ±1.435
2	87.7 ±0.2	0.0	12.3 ±0.2	1.65 ±0.01	93.5 ±0.5	100.2 ±0.8	13.029 ±1.639
3 ^a	82.5 ±0.5	0.0	17.5 ±0.5	1.782 ±0.007	95.9 ±0.5	99.6 ±0.8	3.257 ±0.819
4	72.3 ±0.5	0.0	27.7 ±0.5	4.53 ±0.08	97.0 ±0.5	104.1 ±0.8	17.915 ±1.806
5 ^b	0.0	97.3 ±0.1	2.7 ±0.1	1.73 ±0.05	103.6 ±0.6	118.7 ±0.8	28.810 ±2.381
6	0.0	94.6 ±0.6	5.4 ±0.6	4.41 ±0.05	92.5 ±0.5	107.2 ±0.9	24.559 ±2.136
7	50.6 ±0.3	44.2 ±0.2	5.2 ±0.2	1.85 ±0.01	97.8 ±0.5	108.7 ±0.8	18.729 ±1.887
8	57.5 ±0.2	37.2 ±0.1	5.3 ±0.2	1.561 ±0.007	92.7 ±0.5	107.8 ±0.8	26.448 ±2.298
9	47.6 ±0.4	30.9 ±0.4	21.5 ±0.3	3.21 ±0.02	91.9 ±0.5	97.8 ±0.8	11.074 ±1.396
10	24.9 ±0.1	48.3 ±0.4	26.8 ±0.4	3.44 ±0.03	91.9 ±0.5	94.2 ±0.8	2.475 ±6.56
11	27.0 ±0.5	61.4 ±0.5	11.6 ±0.5	3.85 ±0.03	91.8 ±0.5	98.8 ±0.8	10.244 ±1.394
12 ^a	30.2 ±0.3	63.9 ±0.3	5.9 ±0.3	2.133 ±0.007	93.6 ±0.5	111.6 ±0.8	31.758 ±2465

^a Leakage through the solenoid valve may have biased the composition more than the reported uncertainty.

^b Unable to achieve effervescence.

182

183

184 Measurements 1-5 and 7 allowed the temperature of the liquid mixture and heater surface to
185 stabilize before increasing the heater power as discussed in Section 2. As a result, several of the
186 liquid temperatures were higher than anticipated because the cryocooler was unable to remove
187 the amount of heat that was being added to the liquid by the cartridge heater while maintaining
188 the desired temperature. Measurements 6 and 8-12 rapidly increased the heater power until
189 effervescence occurred.

190
191 Measurements 3 and 10 show a significantly lower heat flux and temperature differential
192 between the heater surface and liquid. Effervescence for measurement 3 was recorded for a very
193 small stream of bubbles coming from a single point on the heater. Measurement 10 was
194 conducted under poor visibility and was determined when there was significant disturbance to
195 the liquid-vapor interface. This could have led to this point being conducted prematurely. Videos
196 of effervescence for each of the data points are publically available to visualize the variability in
197 effervescence for each measurement at <http://hdl.handle.net/2376/12183>. Still images from the
198 video showing effervescence for measurement 11 and 12 are shown in Figure 2.
199



200
201
202 Figure 2. Images of effervescence during measurement 11 (left) and measurement 12 (right).
203

204 Measurements 1, 3, and 12 experienced detectable leakage through the solenoid valve. This
205 could have potentially biased the composition measurement as liquid from the test cell could
206 flow into the liquid trap and vice versa. As a result the uncertainty associated with the
207 composition of these measurements may be higher than the reported values.
208

209 Effervescence was not achieved for measurement 5. The upper voltage limit of the power supply
210 was reached before effervescence occurred. However insight was still gained by measurement 5
211 which showed severe convection currents near the cartridge heater which may have a negative
212 impact on submarine operations and instrument readings. Nonetheless, bubble incipience data in
213 Table 2 are consistent with solubility limits for liquid ethane and liquid methane; due to the
214 lower solubility of nitrogen in ethane, there are fewer bubbles available to come out of solution
215 requiring more heat for bubble incipience. The converse is true for higher liquid methane seas.

216 Furthermore, waste heat flux at bubble incipience is higher at higher pressures and colder liquid
217 temperatures.

218
219 From the Phase 1 Titan Submarine (Hartwig et al., 2016), the waste heat flux into the Titan seas
220 was estimated to be 370 W/m^2 from a detailed thermal balance between radioisotope generator
221 power source, internal insulation, and coolant distribution network. Examination of Table 2
222 shows that the lowest recorded heat flux at the point of bubble incipience is nearly an order of
223 magnitude higher. This implies that the current submarine design has nearly an order of 10 safety
224 factor on the resultant waste heat needed to produce nitrogen bubbles which would interfere with
225 science instruments or propellers.

226

227 **4. Freezing Point Depression Measurements**

228 Upon completion of the effervescence measurements, two freezing point depression
229 measurements were conducted. Though ice buoyancy and formation relevant to Titan has
230 previously been investigated (e.g. Thompson, 1985; Roe and Grundy, 2012; Prokhvatilov and
231 Yantsevich, 1983; Hofgartner and Lunine, 2013), these measurements were necessary to verify
232 predictive models in the literature and to provide experimental data for current Titan sea property
233 models. The same experimental setup was used for the freezing measurements. The experimental
234 procedure was also kept the same except instead of adding heat to achieve effervescence, the test
235 cell and liquid were allowed to continue to cool until ice began to form. The results of the
236 freezing point measurements are presented in Table 3.

237

238

Table 3. Freezing point depression measurements.

Measurement	Methane [mol %]	Ethane [mol %]	Nitrogen [mol %]	Pressure [bar]	Liquid Temp. [K]
F1	61.0 ± 0.1	25.6 ± 0.1	13.4 ± 0.1	0.290 ± 0.007	71.5 ± 0.5
F2	46.9 ± 0.2	45.3 ± 0.1	7.9 ± 0.3	0.517 ± 0.007	74.0 ± 0.5

239

240 The freezing point depression measurements show dramatic subcooling below the triple point
241 temperatures of methane (90.7 K) and ethane (90.4 K) (Lemmon et al., 2013). Freezing point F2
242 was verified visually using the video camera and borescope. A still image of freezing during
243 measurement F2 is shown in Figure 3. The black circle in Figure 3 shows a large white mass of
244 ice in the upper left section of the test cell. The full video is available at
245 <http://hdl.handle.net/2376/12183> and shows the growth of a solid white ice ball within the test
246 cell at a temperature of 74 K and pressure of 0.517 bar.

247



Figure 3. Image of freezing occurring during measurement F2.

248
249
250

251 The first freezing point measurement F1 could not be confirmed visually due to severe fogging
252 on the borescope lens. Instead freezing was determined using the temperature and pressure
253 measurements. The onset of freezing was determined when the pressure stopped decreasing
254 similar to what was observed by Guildner et al. (1976). At the onset of freezing the temperature
255 of the liquid stopped decreasing and stayed constant as the heat extracted by the cryocooler was
256 absorbed by the latent heat of fusion which is responsible for solidification. The pressure and
257 temperature showed similar behavior to freezing point F2.

258

259 The freezing liquid line was depressed more than 15 K below the triple point temperatures of
260 pure ethane. Though there are only two measurements, this data suggests that freezing will occur
261 at higher temperatures for ethane-rich mixtures. This observation is consistent with historical
262 observations.

263

264 5. Conclusions

265 The likelihood of effervescence in a methane-ethane-nitrogen mixture increases with increased
266 nitrogen content. Effervescence in ethane-nitrogen mixtures was only achieved for temperature
267 differences between the submarine surface and liquid greater than 14 K. It was discovered that
268 nitrogen will slowly come out of solution without causing effervescence if heating is done slowly
269 over several minutes. When the heater power was ramped slowly, the pressure in the sealed test
270 cell would continue to rise as the temperature of the liquid increased due to nitrogen coming out
271 of the liquid. Furthermore, the temperature rake measured a significant thermal gradient between
272 liquid below the heater and liquid above the heater. This suggests that heat and bubbles radiating
273 out from the submarine will rise up and away from the submarine. These effects occur at lower
274 heat fluxes and smaller temperature differences between the sea and submarine surface for
275 methane-rich mixtures. Nevertheless, results show that there is an appreciable safety factor on
276 the resultant heat flux into the liquid before the point of bubble incipience for current submarine
277 waste heat fluxes.

278

279 6. Acknowledgments

280 The authors would like to thank Jonathan Lomber of Washington State University for developing
281 the gas composition analysis procedure and providing a brief description of the process. The

282 authors also thank Alex Dunsmoor for conducting the composition measurements. The authors
283 thank Emily Richardson for conducting the video editing. This work was supported by NASA
284 Space Technology Research Fellowship grant NNX14AL59H and NASA research grant
285 NNC16MF93P.
286

287 **References**

288 Corier, D., Garcia-Sanchez, F., Justo-Garcia, D. N. and Liger-Belair, G., "Bubble streams in
289 Titan's seas as a product of liquid $N_2 + CH_4 + C_2H_6$ cryogenic mixture," *Nature Astronomy* **1**,
290 0102 (2017).

291 Guildner, L. A., Johnson, D. P., and Jones, F. E., *J. Res. NBS A Phys. Ch.* **80A**, 505-521 (1976).

292 Hartwig, J. W., Colozza, A., Lorenz, R. D., Oleson, S., Landis, G., Schmitz, P., Paul, M. and
293 Walsh, J., *Cryogenics* **74**, 31-46 (2016).

294 Hartwig, J. W., Meyerhofer, P., Lorenz, R. D., and Lemmon, E. W., "An Analytical Solubility
295 Model for Nitrogen/Ethane/Methane Ternary Mixtures" *Icarus* **299**, 175-186 (2017).

296 Hofgartner, J. D. and Lunine, J. I., *Icarus* **223**, 628-631 (2013).

297 Lemmon, E. W., Huber, M. L. and McLinden, M. O., *NIST Standard Reference Database 23:*
298 *Reference Fluid Thermodynamic and Transport Properties-REFPROP, Version 9.1, National*
299 *Institute of Standards and Technology, Standard Reference Data Program, Gaithersburg.*
300 (2013).

301 Lorenz, R. and Mitton, J., "Titan Unveiled: Saturn's Mysterious Moon Explored", Princeton, NJ,
302 Princeton University Press, 180-250 (2010).

303 Lorenz, R. D., Kirk, R. L., Hayes, A. G., Anderson, Y. Z., Lunine, J. I., Tokano, T., Turtle, E. P.,
304 Malaska, M. J., Soderblom, J. M., Lucas, A., Karatekin, O. and Wall, S. D., "A radar map of
305 Titan Seas: Tidal dissipation and ocean mixing through the throat of Kraken," *Icarus* **237**, 9-15
306 (2014).

307 Malaska, M. J., Hodyss, R., Lunine, J. I., Hayes, A. G., Hofgartner, J. D., Hollyday, G. and
308 Lorenz, R. D., "Laboratory measurements of nitrogen dissolution in Titan Lake fluids," *Icarus*
309 **289**, 94-105 (2017).

310 Mastrogiuseppe, M., Poggiali, V., Hayes, A., Lorenz, R., Lunine, J., Picardi, G., Seu, R.,
311 Flamini, E., Mitri, F., Notarnicola, C., Paillou, P. and Zebker, H., "The bathymetry of a Titan
312 sea," *Geophysical Research Letters* **41 no. 5**, pp. 1432-1437, March 2014.

313 Mitri, G, Showman, A. P., Lunine, J. I. and Lorenz, R. D., "Hydrocarbon lakes on Titan," *Icarus*
314 **186**, 385-394 (2007).

315 Prokhatilov, A. I. and Yantsevich, L. D., *Fiz. Nizk. Temp.* **9**, 185-192 (1983).

316 Richardson, I. A., Hartwig, J. W. and Leachman, J. W., "Experimental PpT-x Measurements of
317 Liquid Methane-Ethane-Nitrogen Mixtures to Support an Extraterrestrial Submarine for Titan,"
318 *Fluid Phase Equilibria* **462**, 38-43 (2018).

319 Richardson, Ian A. *Characterizing Dissolved Gases in Cryogenic Liquid Fuels*. PhD
320 Dissertation, Washington State University. Ann Arbor: ProQuest, 2017.

321 Roe, H. G. and Grundy, W. M., *Icarus* **219**, 733 (2012).

- 322 Stofan, E. R., Elachi, C., Lunine, J. I., Lorenz, R. D., Stiles, F., Mitchell, K. L., Ostro, S.,
323 Soderblom, L., Wood, C., Zebker, H., Wall, S., Janssen, M., Kirk, R., Lopes, R., Paganelli, F.,
324 Radebaugh, J., Wye, L., Anderson, Y., Allison, M., Boehmer, R. and Callahan, P., "The lakes of
325 Titan," *Nature* **445**, 61-64 (2007).
- 326 Taylor, B. N. and Kuyatt, C. E., "Guidelines for Evaluating and Expressing the Uncertainty of
327 NIST Measurement Results," *NIST Technical Note* **1297**, 1-20 (1994).
- 328 Thompson, W. R., "The Atmospheres of Saturn and Titan", *Proc. Int. Workshop. ESA SP-241*,
329 109 (1985).
- 330 Tokano, T. and Lorenz, R. D., "Sun-stirred Kraker Mare: Circulation in Titan's seas induced by
331 solar heating and methane precipitation," *Icarus* **270**, 67-84 (2016).
- 332 Wall, S., Hayes, A., Bristow, C., Lorenz, R., Stofan, E., Lunine, J, Le Gall, A., Janssen, M.,
333 Lopes, R., Wye, L., Sodeblom, L., Paillou, P., Aharonson, O., Zebker, H., Farr, T., Mitri, G.,
334 Kirk, R., Mitchell, K., Notarnicola, C., Casarano, D. and Ventura, B., "Active shoreline of
335 Ontario Lacus, Titan: A morphological study of the lake and its surroundings," *Geophysical*
336 *Research Letters* **37**, p. L05202 (2010).
- 337